

SOME FACTORS AFFECTING THE DESIGN OF A CALORIMETER HOOD AND EXHAUST

Leonard Y. Cooper
Building and Fire Research Laboratory
National Institute of Standards and Technology
Gaithersburg, MD 20899

SUMMARY

This paper considers factors affecting the design of an effective and versatile calorimeter hood and exhaust system. The purpose of the calorimeter, design functions, and inherent limitations of a particular design are discussed. The interactions between the hood structure and the fire and its plume are analyzed in the context of avoiding: flame impingement on the hood; enhanced combustion of a test article, over and above that of a free-burn; loss of combustion product plume gases due to "spill-over" below the hood; and unacceptable dilution of plume gases in the measurement section of the exhaust duct. The concept of the ideally designed hood is introduced, where, throughout the course of the burn of a test article the hood is always immediately above the flame tip and the exhaust rate always exactly matches the hood-ceiling-elevation plume-flow rate. Methods to partially or completely achieve the ideal design are presented. These include the combined features of adjustable hood elevation and adjustable hood exhaust rate.

PURPOSE OF THE CALORIMETER; DESIGN FUNCTIONS; AND SOME INHERENT LIMITATIONS OF A PARTICULAR DESIGN

The combustion product collector or calorimeter hood device is a basic instrument of a fire research laboratory. It is used to study the combustion characteristics of idealized and practical arrays of combustibles under "free burn" conditions, *i.e.*, burning in spaces which are so large and/or so effectively ventilated that for times of interest the burn characteristics of the fuel array are substantially unaffected by the bounding surfaces of the facility that contains the combustibles and/or by any deviations from quiescent, uncontaminated, ambient-temperature air environment that may exist near the combustion zone.

The calorimeter hoods to be considered

This paper is a contribution of the National Institute of Standards and Technology and is not subject to copyright.

here are those which include the design feature of a fan-driven exhaust flow through a duct in the center of the hood. The duct flow rate that would be determined from known exhaust fan characteristics will always be assumed to dominate purely buoyancy-driven flow enhancements. An example of guidance for the design of such a device is presented in Reference 1.

There are two basic functions of the collector hood and its components:

- To collect the combustion products during the entire course of a test and to transport and safely dispose of them outside of the laboratory;
- To measure the characteristics of the combustion products collected by the hood and exhausted through the hood duct, in order to quantify the energy release rate of the fire and the type

and rate of products of combustion generated.

Any particular hood design is limited inevitably in its range of use (*i.e.*, in the range of combustible arrays it can be used to study safely under free burn conditions) by at least four factors:

1. The ability to extract all products of combustion from the laboratory through the hood duct without significant (from the point of view of loss of products of combustion to be measured, or threat of contamination of the laboratory environment) spill-over.
2. The ability to keep the overhead gas smoke temperatures and/or ceiling-or curtain-surface temperatures low enough so that radiation feedback to the fuel array will not be so large as to result in "enhanced burning" (a non-free-burn characteristic).
3. The hood must be elevated enough above the burning combustibles so that the flames do not contact the hood surfaces or enter the hood duct (a non-free-burn characteristic).
4. In terms of useful measurements of energy release rate (from oxygen consumption calorimetry, which is accurate with very few exceptions to within ± 5 percent²) or generation rate of products, the hood should not be so high above the combustion zone, or the amount of outside air that is otherwise mixed with the exhaust should not be so great that excessive dilution of products precludes measurement of their concentrations to satisfactory accuracy.

In terms of a possible guaranteed-free-burn design rule, "the more elevated the hood the better," note that factors 1 and 4 above argue for the lowest possible hood, while factors 2 and 3 argue for the most elevated possible hood.

Note that layer build-up in a hood adds potentially-significant unsteadiness and time delay which distort measurements of, *e.g.*, rate of heat release vs time.

Before a test is actually carried out, one does not generally know whether a particular hood design is suitable for the evaluation of an array of combustibles of interest. This is true since the burn characteristics, *e.g.*, energy release rate, effective elevation and (equivalent "pool") area/diameter of the combustion zone (needed to estimate flame length and plume flow rates and temperatures at the hood/duct-entrance elevation), are *a priori* unknown.

It is the purpose of this paper to study the above issues and to provide recommendations and guidelines for the design of successful calorimeter hood and exhaust systems.

INTERACTIONS BETWEEN THE HOOD, THE FIRE, AND ITS PLUME; DESIGNING TO AVOID "SPILL-OVER"

Basic Phenomena; Criteria to Avoid Spill-Over

The hood's ceiling surface and side-wall skirts, and the duct and its exhaust flow rate involve a variety of interactions with the fire and/or the fire plume. These interactions, analogous to interactions between

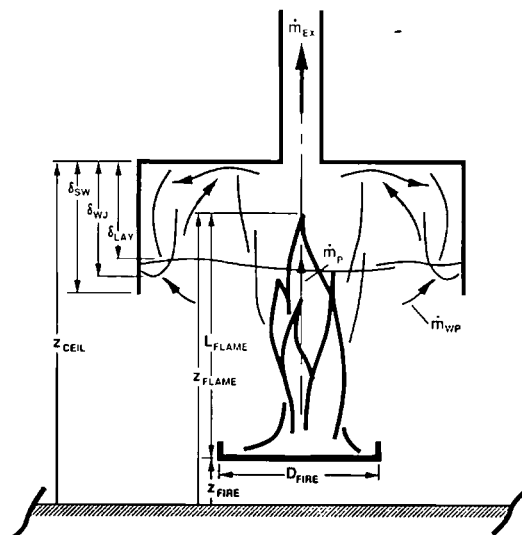


Figure 1. Interactions between the hood components, the fire and its plume.

a fire contained in an enclosed space and the upper surfaces of that space³, are depicted in Figure 1.

The combustion zone itself always interacts with the ceiling and side-walls by way of radiation heat transfer exchanges. A possibly significant aspect of this (in terms of hood-surface-to-fire interactions) is the radiant heating of the exposed ceiling and side-wall surfaces by the high-temperature pyrolyzing surfaces and burning gases of the combustion zone. The radiation absorbed by the hood surfaces can be estimated by assuming that they are totally-absorbing black surfaces being irradiated by a radiating point source (the combustion zone) with strength $\lambda_R \dot{Q}$. Here, \dot{Q} is the total instantaneous energy release rate of the fire, and λ_R is typically of the order of 0.35.

If the hood surfaces are well insulated and the above-mentioned radiation flux from the fire to these surfaces is large enough to yield relatively-high exposed-surface temperatures, in excess, say, of 700–800K, then the re-radiation from the ceiling and side-wall surfaces of the hood to the pyrolyzing surfaces can lead to unacceptable enhanced burning of the combustibles. This can only occur if the solid angle defined by the combustion zone and the hood surfaces is a significant fraction of the total solid angle between the combustion zone and its surroundings.

The portion of the fire energy release rate that is not radiated from the combustion zone, $(1-\lambda_R)\dot{Q}$ is convected away with the buoyant high-temperature gases as they flow upward from the combustion zone. These are driven toward the hood ceiling, entraining ambient air laterally along the way. Thus, a plume of upward-moving elevated-temperature gases, a mixture of all the products of combustion plus entrained air, is formed above the fire.

The hot plume gases impinge on the hood ceiling in the vicinity of the duct. There, the hood duct fan exhausts all or a fraction

of the total plume mass flow rate. If all of the plume gases are not exhausted, the remaining amount turns and spreads out radially across the ceiling surface in a relatively high-temperature, high-velocity, ceiling jet. The ceiling jet traverses the hood ceiling, with convective heat transfer taking place between the gas and the exposed solid surface⁴.

When the ceiling jet reaches the side walls, it impinges on these surfaces and turns downward. A downward-directed wall jet is initiated⁵ and there are associated convective heat transfer exchanges between the gas and the exposed side-wall surfaces⁶. The wall jet is of higher temperature and lower density than the smoke layer or ambient air into which it is being driven. It is therefore retarded in its descent, mainly by the force of buoyancy. Away from the wall surface, material sheds from the wall-jet boundary flow, and this flows back up to the ceiling as an upward-buoyant line-type wall plume, outside and adjacent to the downward wall jet. In its ascent, the wall plume entrains far-field gases laterally. When these wall-plume gases first approach the ceiling, they quickly fill the hood collector to some quasi-steady depth, even as the hood exhaust continues to extract a portion of the primary plume flow. A quasi-steady smoke layer in the hood is established.

As a result of the shedding from the downward wall jet, at some distance below the ceiling its mass flow rate is reduced to zero. This is the penetration distance, δ_{WJ} , of the jet. Let δ_{SW} be the depth of the sidewalls. If the hood is to contain and exhaust all products of combustion, without any spill-over, it is clear that

$$\delta_{SW} \geq \delta_{WJ} \quad (1)$$

Let δ_{LAY} be the depth of the smoke layer in the hood. Then, in terms of a steady-or quasi-steady-state test scenario, the value of δ_{LAY} will be that value which leads to fire-plume and wall-plume rates of inflow to the layer, \dot{m}_p and \dot{m}_{WP} , respectively,

which together exactly balance the mass flow rate of the hood exhaust, \dot{m}_{EX} , i.e.,

$$\dot{m}_{EX} = \dot{m}_P + \dot{m}_{WP} \quad (2)$$

Note that under quasi-steady conditions, if δ_{LAY} is increased, both \dot{m}_P and \dot{m}_{WP} are decreased. Indeed, if the layer submerges the wall jet completely, then $\dot{m}_{WP} = 0$, and all the above-described wall-jet/wall-plume flow activity occurs entirely within the smoke layer itself. Therefore, as expected, the smaller the value of \dot{m}_{EX} , the larger the value of δ_{LAY} .

If the hood is to contain and exhaust all products of combustion, without any spillover, then, in addition to the criterion of Equation 1, it is clear that

$$\delta_{SW} \geq \delta_{LAY} \quad (3)$$

If the smoke layer is opaque and relatively thick, say δ_{LAY} is of the order of 1 m, and is at a relatively high temperature, in excess, say, of 700-800K, then, as in the above-mentioned case of high hood surface re-radiation, the re-radiation from the gas layer to the burning surfaces can lead to unacceptable enhanced burning of the combustibles. Again, this will only occur if the solid angle defined by the combustion zone and the lower smoke layer interface is relatively large.

Even if the layer is thin and gas radiation leading to enhanced burning is not a problem, water cooling of the radiation-exposed hood surfaces (as was used, for example, in Reference 7) should be provided when possible. This is especially true near the duct entrance region where intermittent flame impingement can be anticipated, even under ideal conditions. Cooling of the hood will limit the possible threat of significant radiation feedback to the combustible, leading to enhanced burning. It will also provide for a durable hood structure.

Flame Length; Plume Mass Flow Rate and Temperature

To insure free-burn test characteristics, the top of the flames must not touch the ceiling. To estimate flame length, and thereby determine the suitability of a particular hood design to test a particular class of combustible, it is necessary to characterize the effective elevation, z_{FIRE} , and diameter, D_{FIRE} , of its fire. To do this for geometrically complicated combustibles, like furniture items, and to do so when even qualitative burn characteristics are unavailable, it seems reasonable that one to two (z_{FIRE} , D_{FIRE}) pairs should be considered. The following pair is always recommended:

A z_{FIRE} value which is characteristic of the elevations of the surfaces of the item in its virgin, unburned state. For example, in the case of tables, z_{FIRE} , would be the elevation of the table top; in the case of chairs, the elevation of the top of the seat; in the case of a rectangular slab, the elevation of the top of the slab; etc. A D_{FIRE} is determined from:

$$\pi D_{FIRE}^2 = \text{area of the fire source} \quad (5)$$

where the area of the fire source is taken to be the plan area of the combustible.

If the materials of construction have a propensity to drip, then the following (z_{FIRE} , D_{FIRE}) pair should also be considered:

$$z_{FIRE} = z_{PAN}; \quad \pi D_{FIRE}^2 = \text{area of the pan} \quad (6)$$

where z_{PAN} is the elevation of the pan on which the test item is placed during the burn. Typically, the area of the pan will correspond closely to the plan area of the combustible, and the D_{FIRE} of Equations 5 and 6 will be identical.

Based on a specified (z_{FIRE} , D_{FIRE}) pair, flame length, L_{FLAME} , as measured above z_{FIRE} , can be estimated from Reference 8

$$\begin{aligned} &\text{if } 0.249[(1-\lambda_R)\dot{Q}/\text{kW}]^{2/5} - 1.02D_{\text{FIRE}}/m < 0 \\ &0.249[(1-\lambda_R)\dot{Q}/\text{kW}]^{2/5} - 1.02D_{\text{FIRE}}/m \\ &\text{if } 0.249[(1-\lambda_R)\dot{Q}/\text{kW}]^{2/5} - 1.02D_{\text{FIRE}}/m \geq 0 \end{aligned} \quad (7)$$

where

$$z_{\text{FLAME}} = z_{\text{FIRE}} + L_{\text{FLAME}} \quad (8)$$

corresponds to the elevation which essentially separates the reacting region of the plume, below, from the non-reacting region, above. This is the elevation in the plume where the peak centerline temperature, $T_{P,\text{MAX}}$, is approximately 500K above the ambient.

Using Equation 7, L_{FLAME} vs. $(1-\lambda_R)\dot{Q}$ for different D_{FIRE} were calculated and plotted in Figure 2. These results can be used to estimate the minimum z_{CEIL} for a hood that would be used to exhaust and measure combustion products from a free-burn fire of known elevation, z_{FIRE} , and specified \dot{Q} and λ_R . For example, consider a natural gas burner fire with $D_{\text{FIRE}} = 0.10$ m and $\dot{Q} = 500\text{kW}$. Based on Reference 9, it is reasonable to expect λ_R to be within the range $0.2 < \lambda_R < 0.35$, i.e., $325 \leq (1-\lambda_R)\dot{Q}/\text{kW} \leq 400$. For this fire, L_{FLAME} is estimated from Figure 2 to be in the range $2.4 \text{ m} < L_{\text{FLAME}} < 2.6 \text{ m}$. Therefore, the hood should be no closer to the surface of the

burner than 2.6 m. Alternatively, if, as in the present hood in the NIST Building 205 Fire Research Laboratory, the exhaust duct entry is 2.3 m above the floor (i.e., $z_{\text{CEIL}} = 2.3$ m) and the burner surface is 0.3 m above the floor (i.e., $z_{\text{FIRE}} = 0.3$ m), then the maximum allowable $(1-\lambda_R)\dot{Q}$, $(1-\lambda_R)\dot{Q}_{\text{MAX}}$, is that which produces $L_{\text{FLAME}} \leq 2.0$ m. According to Figure 2, $(1-\lambda_R)\dot{Q}_{\text{MAX}} = 210$ kW. Corresponding to the above λ_R range, the value of \dot{Q} that will lead to $z_{\text{FLAME}} = z_{\text{CEIL}}$ is estimated to be in the range $260 \text{ kW} \leq \dot{Q} \leq 320 \text{ kW}$.

For elevations, z , at and above z_{FLAME} , the mass flow rate of the plume, \dot{m}_p can be estimated from Reference 8.

$$\begin{aligned} \text{For } z - z_{\text{FLAME}} \geq 0: \quad & (9) \\ \dot{m}_p / (\text{kg/s}) &= 0.071[(1-\lambda_R)\dot{Q}/\text{kW}]^{1/3} \\ & \{ (z - z_{\text{FLAME}}) / m + 0.166[(1-\lambda_R)\dot{Q}/\text{kW}]^{2/5} \}^{5/3} \end{aligned}$$

$$\left[\frac{1 + 0.026[(1-\lambda_R)\dot{Q}/\text{kW}]^{2/3} \{ (z - z_{\text{FLAME}}) / m + 0.166[(1-\lambda_R)\dot{Q}/\text{kW}]^{2/5} \}^{-5/3}}{0.166[(1-\lambda_R)\dot{Q}/\text{kW}]^{2/5} \}^{-5/3}} \right]$$

Corresponding to \dot{m}_p , the plume bulk average temperature, T_p , corresponding average density, ρ_p , and volume flow rate, \dot{V}_p , can be estimated from:

$$\begin{aligned} T_p - T_{\text{AMB}} &+ (1-\lambda_R)\dot{Q} / (\dot{m}_p C_p); \quad (10) \\ \rho_p &= \rho_{\text{AMB}} T_{\text{AMB}} / T_p; \quad \dot{V}_p = \dot{m}_p / \rho_p \end{aligned}$$

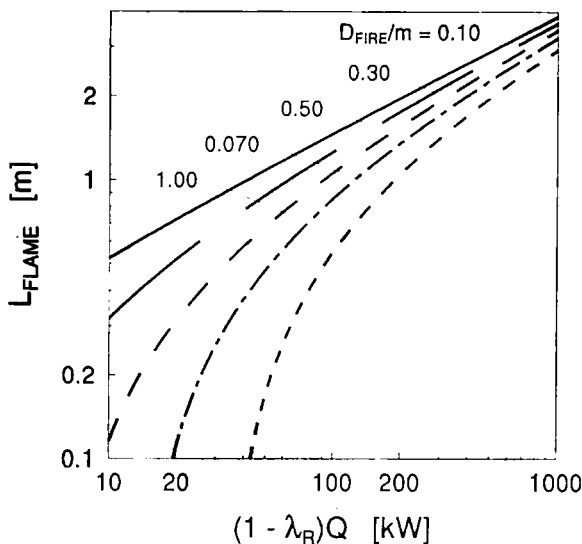


Figure 2. Plots of L_{FLAME} vs. $(1-\lambda_R)\dot{Q}$ for different D_{FIRE} ; from Equation 7.

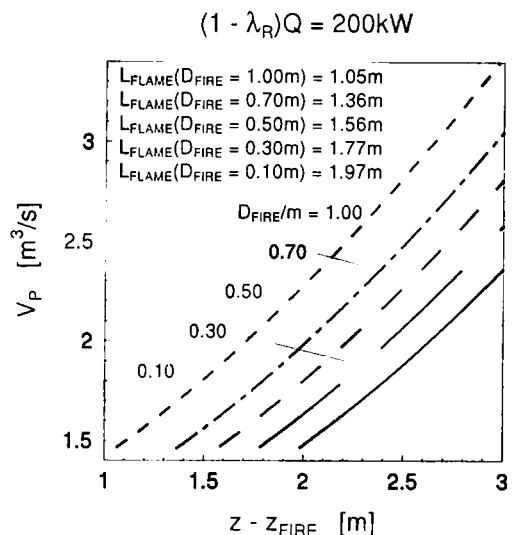


Figure 3. Plots of \dot{V}_p vs. $(z - z_{\text{FIRE}}) > L_{\text{FLAME}}$, for $(1-\lambda_R)\dot{Q} = 200\text{kW}$ and for different values of D_{FIRE} ; from Equations 7-10.

In an example application of Equations 8-10, for different values of D_{FIRE} , \dot{V}_P was calculated for $(1-\lambda_R)\dot{Q} = 200 \text{ kW}$ as a function of $z - z_{\text{FIRE}} > L_{\text{FLAME}}$. The results are presented in Figure 3. From this figure, it can be determined, for example, that for a pool fire 2 m below the NIST hood, *i.e.*, 0.3 m above the floor, the value of $\dot{V}_{P,\text{CEIL}} = \dot{V}_P(z = z_{\text{CEIL}})$ ranges from 1.5 m³/s for $D_{\text{FIRE}} = 0.10 \text{ m}$ to 2.3 m³/s for $D_{\text{FIRE}} = 1.0 \text{ m}$. Since the present NIST hood system can exhaust up to 2.2 m³/s (a flow speed of 12 m/s through the 0.48 m diameter duct¹⁰), the system may be able to (almost) exhaust all of the plume flow for these relatively small fires.

The following property values were used in the calculations of Figure 3, and will be used below in all calculations to follow:

$$\rho_{\text{AMB}} = 1.2 \text{ kg/m}^3; C_p = 1 \text{ kW s/(kgK)}; T_{\text{AMB}} = 300 \text{ K.}$$

The values of \dot{m}_P , T_P , ρ_P , and \dot{V}_P at $z = z_{\text{FLAME}}$ are designated as $\dot{m}_{P,\text{FLAME}}$, $T_{P,\text{FLAME}}$, $\rho_{P,\text{FLAME}}$, and $\dot{V}_{P,\text{FLAME}}$, respectively. From Equations 9 and 10, these are seen to be independent of D_{FIRE} and given by

$$\begin{aligned} \dot{m}_{P,\text{FLAME}} &= 0.0054(1-\lambda_R)(\dot{Q}/\text{kW})\text{kg/s}; \\ T_{P,\text{FLAME}} - T_{\text{AMB}} &= 1./[0.0054C_p\text{kg}/(\text{kWs})] = 185 \text{ K}; \\ \rho_{P,\text{FLAME}} &\approx 0.74 \text{ kg/m}^3; \\ \dot{V}_{P,\text{FLAME}} &\approx 0.0073(1-\lambda_R)(\dot{Q}/\text{kW})\text{m}^3/\text{s} \end{aligned} \quad (11)$$

As an example application of Equation 11, consider the above case of the $(1-\lambda_R)\dot{Q} = 200 \text{ kW}$, 0.10 m-diameter, natural gas fire which was determined to have a 2.0 m flame length. Equation 11 again provides the estimate that $\dot{V}_{P,\text{FLAME}} = 1.5 \text{ m}^3/\text{s}$ for this fire. It is therefore concluded that near the flame tip, for this fire the present capability of the NIST hood exhaust system should be adequate to exhaust the entire plume flow.

Using the Point Source Plume for Elevations Above The Flame

For elevations somewhat above the top of the flame and higher, *i.e.*, above the elevation where $T_{P,\text{MAX}} > 500 \text{ K} + T_{\text{AMB}}$, and to a level of accuracy appropriate to certain aspects of hood design analysis, the fire plume can be characterized by the properties of a point-source-driven plume of strength $(1-\lambda_R)\dot{Q}$ ¹¹. Such properties are independent of D_{FIRE} ¹¹. For this reason, in the analysis to follow it is more convenient to use the point-source plume description than the description of Equations 7-10, which does depend on D_{FIRE} .

For $T_{P,\text{MAX}} = T_{\text{AMB}}(1+9.1\dot{Q}^{*2/3}) > 500 \text{ K} + T_{\text{AMB}}$, corresponding to

$$\begin{aligned} 1) \quad \dot{Q}^* &< [(500 \text{ K}/T_{\text{AMB}})/9.1]^{3/2} = 0.078; \text{ or} \\ 2) \quad z - z_{\text{FIRE}} &> \{[9.1(1-\lambda_R)\dot{Q}]/[\rho_{\text{AMB}}C_p(500 \text{ K})g^{1/2}]\}^{2/5} \\ &\approx 0.12[(1-\lambda_R)\dot{Q}/\text{kW}]^{2/5} \text{ m}; \\ \dot{m}_P / (\text{kg/s}) &= 0.21\rho_{\text{AMB}}g^{1/2}(z - z_{\text{FIRE}})^{5/2}\dot{Q}^{*1/3} \\ &\approx 0.79[(z - z_{\text{FIRE}})/\text{m}]^{5/2}\dot{Q}^{*1/3} \end{aligned} \quad (12)$$

where $g = 9.8 \text{ m/s}^2$,

$$\begin{aligned} \dot{Q}^* &= (1-\lambda_R)\dot{Q}/[\rho_{\text{AMB}}C_pT_{\text{AMB}}g^{1/2}(z - z_{\text{FIRE}})^{5/2}] \\ &\approx 8.9(10^{-4})(1-\lambda_R)(\dot{Q}/\text{kW})/[(z - z_{\text{FIRE}})/\text{m}]^{5/2} \end{aligned} \quad (13)$$

and where, with the use of Equation 10, T_P , ρ_P , and \dot{V}_P can be calculated from Equations 12 and 13.

Using Equations 10, 12, and 13, values of \dot{V}_P vs $(1-\lambda_R)\dot{Q}$ for different $(z - z_{\text{FIRE}})$ were calculated and plotted in Figure 4. The figure can be used to estimate $\dot{V}_{P,\text{CEIL}}$ and, therefore, the minimum exhaust flow rate that would avoid any hood filling and spillover. For example, aside from maximum flame length requirements, it is found from Figure 4 that for the existing NIST hood structure, with $z_{\text{CEIL}} = 2.3 \text{ m}$, an increased exhaust capacity, up to approximately 5 m³/s, is required if the facility is to be able to test pool fires, 0.3 m above the floor,

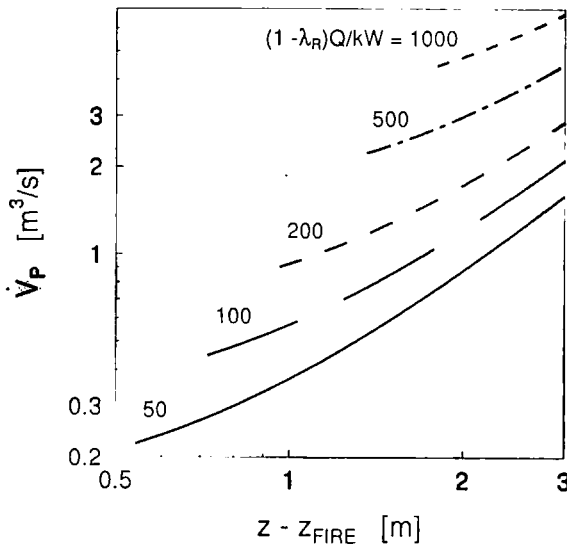


Figure 4. Plots of \dot{v}_p vs $(z - z_{FIRE})$, where $T_{p,MAX} \leq T_{AMB} + 500K$ for different values of $(1 - \lambda_R)Q$; from the point source plume model of Equations 10, 12, and 13.

with convected plume enthalpy flows as high as 1000 kW. Note that for typical values of $\lambda_R = 0.35$ or greater, this corresponds to fires with \dot{Q} of 1500 kW or greater.

An Estimate of Required Side-Wall Depth

It has been shown in Reference 5 that for room fire scenarios with no directly-overhead plume exhaust (*i.e.*, all ceiling venting is from vents which are removed from the plume/ceiling impingement point), the depth of the wall jet is generally comparable to the fire-to-ceiling distance. In the present application, this suggests that hood side-walls, properly designed according to the criterion of Equation 1, may obstruct required visualization of the burning test article. Thus, relatively independent of the size of \dot{Q} , and for "typical" full-scale fires" with no ceiling flame impingement,

$$\delta_{WJ}/H \approx 0.8; \quad H = z_{CEIL} - z_{FIRE} \quad (14)$$

It is also shown in Reference 5, again for room fire scenarios with no directly-centered plume exhaust, that \dot{m}_{WP} (for the case of negligible δ_{LAY}) are very large indeed, 10 or more times \dot{m}_p .

In view of the above, it is evident that the

effect of the hood's direct plume exhaust, which reduces the limiting-large δ_{WJ} estimate of Equation 14, must be considered in determining a minimum acceptable design value for side wall depth.

Required Side-Wall Depth; the Effect of Direct Plume Exhaust.

In the analysis and discussion to follow, it is assumed that the exhaust duct inlet is centered exactly along the plume axis so that, unless the exhaust mass flow is greater than the plume mass flow, $\dot{m}_{EX} / \dot{m}_{P,CEIL} > 1$, the inlet flow is drawn only from the plume flow (*i.e.*, no component of the inlet flow is drawn asymmetrically from the outside ambient environment). This assumption and its practical implications will be discussed below.

In the immediate region of the plume/ceiling impingement point, it is assumed that the hood duct exhausts of the plume gases. The temperature of the exhausted flow is assumed to be equal to the bulk average temperature of the plume at the ceiling elevation, $T_{P,CEIL} = T_P(z = z_{CEIL})$. The remaining flow, has a mass flow rate

$$\dot{m}_{EQ} = \dot{m}_{P,CEIL} (1 - \dot{m}_{EX} / \dot{m}_{P,CEIL}) \quad (15)$$

and average temperature $T_{P,CEIL}$, where $\dot{m}_{P,CEIL} = \dot{m}_p(z = z_{CEIL})$. When it impinges on the ceiling, this flow turns horizontally and is assumed to flow radially outward along the exposed surface of the hood ceiling, uniformly distributed in a radially symmetric ceiling jet flow.

We now seek the properties of an equivalent point source of buoyancy of strength \dot{Q} (to be determined) located along the original plume axis at an elevation \dot{m}_{EQ} (to be determined) where the characteristics of the equivalent source are such that upon impinging on a ceiling surface it will generate the ceiling jet of mass flow rate, \dot{m}_{EQ} , at average temperature, $T_{P,CEIL}$. From Equations 12 and 13, it is found that z_{EQ} must satisfy:

$$\begin{aligned} \dot{m}_{EQ} &= 0.21 \rho_{AMB} g^{1/2} (z_{CEIL} - z_{EQ})^{5/2} \dot{Q}_{EQ}^{*1/3} \\ \dot{Q}_{EQ}^{*} &= (1 - \lambda_R) \dot{Q} / [\rho_{AMB} C_P T_{AMB} g^{1/2} (z_{CEIL} - z_{FIRE})^{5/2}] \\ &= \dot{Q}_{EQ} / [\rho_{AMB} C_P T_{AMB} g^{1/2} (z_{CEIL} - z_{EQ})^{5/2}] \end{aligned} \quad (16)$$

Solving Equation 16 for \dot{Q}_{EQ} and z_{EQ} leads to:

$$(z_{CEIL} - z_{EQ}) / (z_{CEIL} - z_{FIRE}) = (1 - \dot{m}_{EX} / \dot{m}_{P,CEIL})^{2/5} \quad (17)$$

$$\dot{Q}_{EQ} / [(1 - \lambda_R) \dot{Q}] = 1 - \dot{m}_{EX} / \dot{m}_{P,CEIL} \quad (18)$$

With the results of Equations 17 and 18, it is now possible to estimate the δ_{WJ} due to the ceiling jet of the unexhausted plume flow. This is done by simulating the flow as a ceiling jet driven by the plume of the equivalent buoyant point source, and by using Equation 14 with $H = z_{CEIL} - z_{EQ}$.

It is easy to see that even when a significant fraction of plume flow is exhausted, the resulting reduction of δ_{WJ} is not large enough to reduce significantly the effect of spill-over in practical hood designs. For example, with $z_{CEIL} - z_{FIRE} = 2$ m and $\dot{m}_{EX} / \dot{m}_{P,CEIL} \ll 1$ (i.e., a relatively small hood exhaust), Equations 1 and 12-14 lead to the likely-unacceptable side-wall length requirement, $\delta_{SW} \geq \delta_{WJ} \approx 0.8 (2.0 \text{ m}) = 1.6$ m. However, by exhausting, say, 75 percent of $\dot{m}_{P,CEIL}$ the side-wall length requirement is only reduced to $\delta_{SW} \geq \delta_{WJ} \approx 0.8 (2.0 \text{ m}) (1 - 0.75)^{2/5} = 0.9$ m. It is therefore concluded that a successful hood design, where δ_{SW} is no more than a small fraction of $z_{CEIL} - z_{FIRE}$, requires the duct exhaust flow to exceed the plume flow at the hood ceiling height.

For any particular hood design and burn test item, an exact match between \dot{m}_{EX} and $\dot{m}_{P,CEIL}$ would lead to an "ideal" design operating condition in the sense that concentration of products in the hood duct flow would be maximized and, as a result, the highest possible accuracy in their measurement could be attained. A higher exhaust rate would lead to further dilution of products in the duct, and a smaller

exhaust would lead to hood filling and, possibly, spill-over.

AN IDEAL DESIGN: HOOD AT FLAME TIP; EXHAUST RATE MATCHES EXACTLY THE CEILING PLUME FLOW RATE

For a hood of specified ceiling height, flame length considerations place an absolute constraint on the test items that can be properly tested in it (see the third of the limiting factors of hood design listed on page 100). Similarly, in contemplating design of a new hood, the minimum acceptable value of hood ceiling height would be determined by the expected flame lengths of the class of burn test items for which the facility is being designed.

The following are the characteristics of a hood of ideal design:

1. The hood height is adjustable over the widest possible range. The hood ceiling elevation is always maintained slightly above the flame tip of the free-burning test item (i.e., to maximize product concentration in the plume at the elevation of the exhaust duct while meeting the basic free-burn constraint).
2. The hood exhaust flow rate is adjustable over the widest possible range. The exhaust flow rate is always maintained at the minimum value that completely exhausts the plume flow and eliminates any smoke layer in the hood (i.e., to maximize the product concentration in the duct, thereby yielding the highest possible accuracy in measured energy release and product generation rates.)

These ideal hood features and their implementation are discussed as follows.

The Adjustable-Hood-Height Feature

Achieving the adjustable-hood-height feature. The adjustable hood height fea-

ture is for the purpose of obtaining control of the fire-to-ceiling distance. Such control can be achieved by raising and lowering either the test item or the hood. Of these two methods, the one involving movement of the test item is the less practical. It would require a platform on which is mounted the burning test item, all photography equipment, and other instruments. It would pose great—and possibly insurmountable—difficulties for proper visualization by the test personnel.

A design concept involving raising and lowering the hood is achievable and practical. One possible way to implement the concept is portrayed in Figure 5. The idea is to support the hood by chain or cable from a motor mounted on the ceiling. The centering of the hood above the axis of the fire plume would be maintained by guide-cables or guide-rails, much like an elevator. The constraining feature of this concept is that possible leak points upstream of any in-duct measurement station(s) only involve relatively small rates of inflow of ambient air. One possible implementation of the adjustable-height hood is depicted in Figure 5. This involves a relatively-large-diameter, high-temperature-resistant, accordion-like, metal duct material.

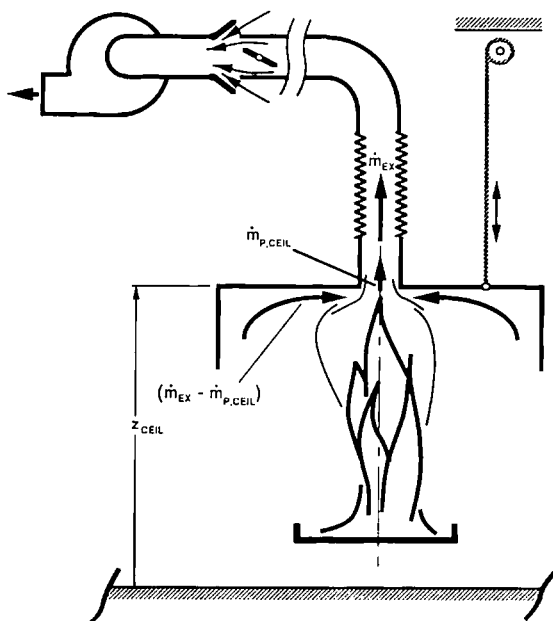


Figure 5. A possible implementation of the ideal hood design concept with adjustable— z_{CEIL} and \dot{m}_{ex}

Implementing the adjustable-hood-height feature. The adjustable-hood-height feature can be implemented in either a technically advanced or a more conservative manner.

The more conservative implementation involves a test procedure where, based on estimates of the effective values of $D_{\text{FIRE}}(s)$, $z_{\text{FIRE}}(s)$, λ_R , and \dot{Q} , the test personnel would first determine (*e.g.*, from Figure 2) the maximum flame tip elevation to be expected during the course of the free burn of a specific test item. The hood height would then be set accordingly and fixed for the entire test run.

In using this approach, the hood configuration would be optimized, in principle, at the time of peak flame-tip elevation. However, as mentioned earlier, for practical assemblies of combustibles the ability to make accurate *a priori* estimates of fire characteristics, and, therefore, of flame tip elevation is usually very limited.

A more advanced implementation of the adjustable-hood-height feature involves a test procedure where hood height adjustments are made during the course of a test burn, with the hood “following” the flame tip as it grows, fluctuates, and then decays. Using the simpler of two possible approaches, hood height corrections would be made manually according to flame-tip visualization by the test personnel. In a more advanced approach, hood height corrections would be made by monitoring flame tip elevation automatically, say with a flame radiation detector, and by providing appropriate automatic feedback control to the hood-support cable motor. Thus, in an optimum way, z_{CEIL} would be maintained close to the flame tip, during (most of) the entire test run.

Achieving and Implementing the Adjustable-Hood-Exhaust-Flow Feature

The adjustable-hood-exhaust-flow feature can be achieved with a variable-speed fan. It can also be achieved with a fixed-speed fan implemented with a duct side-vent having

a motor-controlled variable area. Also, the side vent would be combined with an upstream, motor-controlled, duct damper. (The fan/vent/damper system would be located downstream of the duct measurement station.) The purpose of the side vent would be to allow outside air to be drawn to the inlet side of the fan, thereby reducing the portion of the fan inlet flow exhausted through the duct (*i.e.*, reducing \dot{m}_{EX}). With the side vent in a fully open position, the damper would be used to reduce the \dot{m}_{EX} exhaust flow to arbitrarily small values. This feature would allow testing of relatively-small- \dot{Q} fires, with correspondingly small values of $\dot{m}_{P,CEIL}$ and $\dot{V}_{P,CEIL}$ at the flame tip elevation.

Figure 5 depicts the fixed-speed fan system

THE ASSUMPTION OF A CENTERED HOOD DUCT INLET

It has been assumed above that the exhaust duct inlet of the hood is centered exactly along the plume axis and that, unless $\dot{m}_{EX} > \dot{m}_{P,CEIL}$, all flow drawn through the exhaust duct is extracted from the plume flow itself. In practice the plume at the ceiling elevation is never exactly centered. Also, the plume is never exactly rotationally symmetric. Especially if $\dot{m}_{EX} \approx \dot{m}_{P,CEIL}$, it is inevitable that some of the mass of material included in \dot{m}_{EX} is drawn initially from the quiescent ambient air. Then, the portion of $\dot{m}_{P,CEIL}$ not immediately exhausted must flow sideways, producing local ceiling-jet flow activity. This, in turn, leads to some smoke-filling of the hood and possibly some "preferred-direction" spill-over, etc. In general, a complicated three-dimensional, unsteady flow is established near the hood exhaust duct entrance. The characteristics of this flow would be peculiar to the particular burn item being tested, the shape of the hood, etc.

The undesirable and essentially unacceptable phenomenon of side-flow leading to spill-over can be eliminated by increasing

$\dot{m}_{EX} > \dot{m}_{P,CEIL}$. It is also possible that the phenomenon can be suppressed by optimizing the shape of the hood.

In view of the complicated fluid dynamics involved, it is not possible to quantify simply and with full generality the extent to which increases in \dot{m}_{EX} are required to eliminate spill-over related to the centered hood/duct-inlet problem for a particular hood design. It is also difficult to quantify the importance of the shape of the hood to the side-movement/spill-over phenomenon. For example, referring to Figure 6, for a given hood depth and span, it is not clear whether a cone-type configuration is to be preferred over a design involving a flat ceiling hood with vertical side vents. (The latter being the basic shape of the present NIST hood.)

Prior to the establishment of hood shape guidelines, it is necessary to quantify the centered hood/duct-inlet problem as it relates to the hood design shape. For an existing hood this can be done quickly and simply with a series of gas burner tests. The objective of such a test program would be to establish the values of $\dot{m}_{EX} > \dot{m}_{P,CEIL}$, as a function of $\dot{m}_{P,CEIL}, (1-\lambda_R)\dot{Q}$, and plume off-set, required to exactly exhaust all of $\dot{m}_{P,CEIL}$,

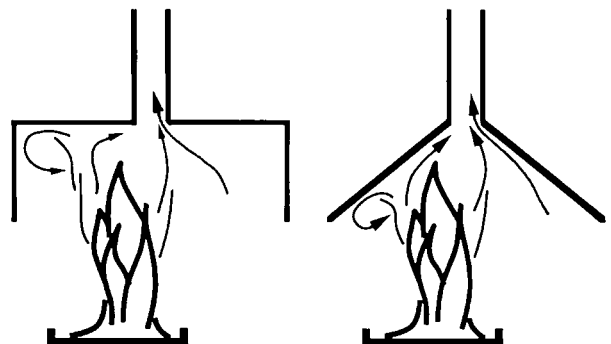


Figure 6. Sketch of the flow for an off-center plume in hoods with identical depth and span and with adequate $\dot{m}_{EX}/\dot{m}_{P,CEIL} > 1$ to achieve full exhaust of the plume flow, without a smoke-layer: left - horizontal hood ceiling with side-walls; right - conical hood.

or at least to ensure no plume-product spill-over from the hood. Hopefully, it would be determined in such a test program that, for the expected plumes of burning test items for which the hood assembly is being designed, these $\dot{m}_{EX} > \dot{m}_{P,CEIL}$ values are not too much greater than 1. If such is not the case, and if the product-dilution problem is considered significant, then an additional hood-shape design effort would be required prior to the establishment of a successful overall hood/exhaust system design.

GENERAL RESULTS AND GUIDELINES; GENERAL CONCLUSIONS

General Results and Guidelines

The following general results and guidelines have been developed for the design of an ideal combustion product calorimeter hood/collector and exhaust:

1. The elevation of the hood should always be maintained at or above the flame tip [the elevation of the latter is determined from Equation 7 or Figure 2]. Keeping the hood elevation near the flame tip will make it possible to exhaust the hood at a rate that maximizes the concentrations of products of combustion in the measurement section of the duct, thereby leading to the highest possible accuracy in the measurement of the fire's energy release rate and the product generation rates.
2. It is not practical to depend on the depth of hood side-walls to eliminate plume-product spill-over from the hood; the elimination of spill-over can be accomplished effectively and economically by increasing the hood exhaust flow rate capability, albeit at the expense of reduction in species concentration at the point of measurement. If this is not possible, then the measurement capability of an existing hood should be appropriately "derated," *i.e.*, relative to acceptable test items whose free burn

characteristics can be evaluated in the hood facility.

3. The exhaust rate of the hood duct flow, \dot{m}_{EX} , should be the smallest possible value that would lead to direct extraction of all the flow in the fire plume, $\dot{m}_{P,CEIL}$ [determined from Equation 9 and Figure 3, or from Equations 12 and 13 and Figure 4], *i.e.*, as the plume impinges on the ceiling of the hood at or near the duct entrance.
4. To accomplish item 3, \dot{m}_{EX} will always have to exceed $\dot{m}_{P,CEIL}$. For a particular hood design, a determination of $\dot{m}_{EX} > \dot{m}_{P,CEIL}$ required to accomplish the exhaust objective of item 3 would require a limited experimental program involving burns with a well-characterized fire source and with known, measured offsets between the plume and the duct axis. A quality hood design is one which can meet the exhaust criterion of item 3 with values of $\dot{m}_{EX} > \dot{m}_{P,CEIL}$ which are not significantly greater than 1, even when there is a moderate offset between the plume and the duct axes.
5. An ideal hood exhaust design is one that can meet all of the above guidelines continuously, or at least at critical times, during the course of a free-burn test. This can be accomplished, for example, with the use of a hood exhaust system which uses (a) an adjustable-elevation hood collector and a variable-speed fan, or (b) a relatively-large-capacity fixed-flow fan (Figure 5) with an adjustable-area side-vent in the duct and an adjustable duct damper, all of which would be located downstream of the duct measurement section.
6. Water cooling of the hood structure should be provided where possible. This will limit the possibility of significant radiation feedback to and enhanced burning of the combustibles. It will also provide for a more durable hood structure.

General Conclusions

Prior to actual testing, it is not possible to know the free-burn characteristics of practical test articles to the point that ideal hood/

exhaust design parameters can be established. Nevertheless, by use of the proposed methods of continuous manual or automatic control and for relatively broad bounds of test article burn characteristics, the ideal hood/exhaust design concepts proposed here should be capable of providing measurements at near-optimum accuracy throughout most of the test run. The ideal hood/exhaust design concept would yield a versatile test instrument that would be a valuable addition to any fire test laboratory.

ACKNOWLEDGEMENTS

The author acknowledges gratefully Mr. Emil Braun and Dr. Thomas Ohlemiller for useful discussions on past and current use of the NIST furniture calorimeter and on future needs of this facility.

NOMENCLATURE

C_p specific heat at constant pressure, 1 kWs/(kgK)

D_{FIRE} effective area of the fire, Figure 1

g acceleration of gravity

H fire-to-hood distance, Equation 14

L_{FLAME} flame length, Figure 1

\dot{m} mass flow rate

\dot{m}_P \dot{m} of plume at elevation of the layer interface, Figure 1

$\dot{m}_{P,CEIL}$ \dot{m} of plume at z_{CEIL}

$\dot{m}_{P,FLAME}$ \dot{m} of plume at z_{FLAME}

\dot{m}_{WP} \dot{m} of ambient entrained into wall plume, see Figure 1

\dot{m}_{EQ} \dot{m} of equivalent source, Equations 15 and 16

\dot{m}_{EX} \dot{m} of hood exhaust

\dot{Q} total instantaneous energy release rate of the fire

\dot{Q}_{EQ} \dot{Q} of equivalent source, Equation 16

\dot{Q}^* dimensionless \dot{Q} , Equation 13

T absolute temperature

T_{AMB} T of ambient, 300 K

T_P bulk average T of plume

$T_{P,CEIL}$ T_P at z_{CEIL}

$T_{P,FLAME}$ T_P at z_{FLAME}

$T_{P,MAX}$ peak centerline temperature of the plume

\dot{V}_P volume flow rate of the plume, Equation 10

$\dot{V}_{P,FLAME}$ \dot{V}_P at z_{FLAME}

z distance above a reference elevation

z_{CEIL} z of hood ceiling, Figure 1

z_{EQ} z of equivalent source, Equation 17

z_{FIRE} z of fire, Figure 1

z_{FLAME} z of flame tip, Equation 8, Figure 1

z_{PAN} z of pan supporting test item

δ_{LAY} depth of the layer interface

δ_{SW} depth of the sidewalls

δ_{WJ} penetration depth of the wall jet

λ_R fraction of \dot{Q} radiated from the combustion zone

ρ density

ρ_{AMB} ρ of ambient, 1.2kg/m³

ρ_P ρ corresponding to T_P , Equation 10

REFERENCES

1. "Standard Test Method for Fire Testing of Real Scale Upholstered Furniture Items," ASTM E 1537 - 93, 1993 *Annual Book of ASTM Standards*, Section 4, ASTM, Philadelphia, pp. 1202-1219, 1993.
2. Janssens, M. and Parker, W.J., "Oxygen Consumption Calorimetry," Chapter 3 of *Heat Release in Fires*, Babrauskas, V. and Grayson, S.J., eds., Elsevier, pp. 31-59, 1992.
3. Cooper, L.Y., "Smoke Movement in Rooms of Fire Involvement and Adjacent Spaces," *Fire Safety Journal*, Vol. 7, pp. 33-46, 1984.
4. Cooper, L.Y., "Convective Heat Transfer to Ceilings Above Enclosure Fires," *19th Symposium (International) on Combustion*, Combustion Institute, pp. 933-939, 1982.
5. Cooper, L.Y., "Ceiling Jet-Driven Wall Flows in Compartment Fires," *Combustion Science and Technology*, Vol. 62, pp. 285-296, 1988.
6. Cooper, L.Y., "Heat Transfer in Compartment Fires Near Regions of a Ceiling-Jet Impingement on a Wall," *Journal of Heat Transfer*, Vol. 111, pp. 455-460, 1989.
7. Babrauskas, V., Lawson, J., Walton, W., and Twilley, W., "Upholstered Furniture Heat Release Rates Measured with the Furniture Calorimeter," NBS-IR 82-2604, National Institute of Standards and Technology, Gaithersburg MD, 1982.
8. Heskestad, G., "Engineering Relations for Fire Plumes," *Fire Safety Journal*, Vol. 7, pp. 25-32, 1984.
9. McCaffrey, B.J., "Some Measurements of the Radiative Power Output of Diffusion Flames," *Proceedings of 1981 Meeting of Western States Section of Combustion Institute*, paper WSS/CI 81-15, 1981.
10. Braun, E., private communication, NIST, Gaithersburg MD, 1993.
11. Zukoski, E.E., Kubota, T., and Cetegen, B., "Entrainment in Fire Plumes," *Fire Safety Journal*, Vol. 3, pp.107-121, 1980/81.